

Düzce University Journal of Science & Technology







Dielectric, UV-vis, FTIR Spectroscopic and Rheological Studies on the Quality of Traditional Homemade Vinegars

DOrhan YALÇIN ^a, Muhittin ÖZTÜRK ^b, DÖmer GÖRGÜLÜER ^{a,*}, Mahmut AYDIN^c

- ^a Department of Physics, Niğde Ömer Halisdemir University, 51240, Niğde, Türkiye
- ^b Program of Opticianry, Niğde Ömer Halisdemir University, 51200, Niğde, Türkiye
- ^c Institute of Science, Niğde Ömer Halisdemir University, 51240, Niğde, Türkiye
- * Corresponding author's e-mail address: ogorguluer@ohu.edu.tr

Article information:

Received: 25/12/2024, Revision: 16/04/2025, Accepted: 03/06/2025

DOI: 10.29130/dubited.1607245

ABSTRACT

This study aimed to determine the quality differences of the apple, blended apple, grape, blended grape, hawthorn and blended hawthorn homemade vinegars produced by the traditional method. These vinegars were analyzed by using a combination of the dielectric spectroscopy, UV-vis spectroscopy, Fourier transform infrared spectroscopy and rheological techniques. Dielectric properties were analyzed as frequency dependent and behaviors consistent with Maxwell-Wagner theory were demonstrated. The complex impedance plane plots corresponding to the impedance circuit on the Smith chart, which is the equivalent resistor-capacitor (RC) circuit for vinegar, were found to be compatible with the Cole-Cole relaxation model. It was determined that the UV-vis spectra of vinegars differ depending on the concentration of organic acids and phenolic compounds in their content. By obtaining the optical band gaps (E_g) for all samples, we observed that most blended vinegars had lower the E_g values than pure ones. According to flow behaviours, it was revealed that all vinegars whose quality characteristics we analyzed, have non-Newtonian shear-thickening (dilatant) fluid behavior.

Keywords: Dielectric Spectroscopy, UV-Vis Spectroscopy, FTIR Spectroscopy, Vinegar, Rheology

I. INTRODUCTION

Vinegar is one of the oldest known beverages. The oldest records about vinegar date back to BC. The Babylonians produced vinegar using dates in 5000 BC and used it for pickling and preserving food (Bottéro, 2004). Throughout history, vinegars have been used as a preservative in food, a medical material such as primitive antibiotics, cleaning materials, etc. for many other purposes.

Vinegar is produced by a two-stage fermentation process in which fermentable sugar is converted to ethanol by yeasts in the first stage and ethanol is converted to acetic acid mostly by Acetobacter bacteria in the second stage (Adams, 1998). Although the production method of vinegar was limited in the past, nowadays vinegar is produced by many different methods. Vinegars are produced by two types of methods: slow type vinegar production, such as traditional, Orleans and Pasteur methods, and fast type vinegar production, such as Generator and Submerged methods (Bourgeois & Barja, 2009).

In recent years, many studies have been carried out revealing the health benefits of vinegar (Ho et al. 2017; Entani et al., 1998; Chen et al., 2016; Budak et al., 2014). The antioxidant activity of phenolic compounds in vinegar is very important for human health. In the studies carried out so far, the most detected organic acids and phenolic compounds in fruit vinegars are gallic acid, protocatechuic acid, chlorogenic acid, caffeic acid, p-coumaric acid, tartaric acid, malic acid, lactic acid, citric acid, and succinic acid (Liu et al., 2019).

The quality of vinegar is its most important feature in terms of both its health benefits and its commercial market and it is determined by many factors such as the material from which it is made, the phenolic compounds it contains and the fast or slow production process.

Many analysis techniques are used to determine the quality of vinegar such as high-performance fluid chromatography (HPLC) (Cheng et al., 2020), gas chromatography-mass spectrometry (GC–MS) method (Ubeda et al., 2011), inductively coupled plasma mass spectrometry (ICP–MS) (Londonio et al., 2019), graphite furnace atomic absorption spectrometry (GFAAS) (de Oliveira & Neto, 2007), Fourier transform infrared spectroscopy (FTIR) (Guerrero et al., 2010; Öztürk, 2021a, 2021b), ultraviolet-visible (UV-vis) spectroscopy and rheology methods (Öztürk, 2021a, 2021b; Yalçın et al., 2021; Öztürk et al., 2022).

In the scope of this work, we have conducted analysis of six different traditional homemade vinegars (apple, blended apple, grape, blended grape, hawthorn and blended hawthorn) using the dielectric spectroscopy, UV-vis spectroscopy, FTIR spectroscopy and rheological techniques. Furthermore, we have compared the analysis results of the vinegar obtained purely from the same type of fruits with the vinegar obtained by adding chickpea, cracked wheat and granulated sugar before the fermentation processes. In addition, quantum effects resulting from photon energy and band gaps were investigated for organic acid molecules in vinegar. The polarization mechanisms that determine the dielectric parameters of vinegars are discussed depending on frequency. Moreover, the compliance for all samples with dielectric relaxation models was examined and its relationship to the impedance circuit on the Smith chart was determined. Thus, for the first time in a study, six homemade vinegars were analyzed using three spectroscopic techniques along with rheological methods and as a result of these analyses, quality differences among the vinegars were identified.

II. MATERIALS AND METHODS

A. Production of Vinegars

Within the scope of this study, the fruits used in the production for all vinegars were grown completely organically without using any chemicals or pesticides and harvested from their natural environment at maturity stages. In order to get rid of harmful bacteria that may be on all fruits, they were kept in glass containers filled with 5% apple vinegar and 95% clean spring water for about three hours. Then, 2 kg of each fruit variety was taken and other stages were started for the production of traditional homemade vinegars.

First, the apples are chopped into small pieces, the hawthorn and grape fruits are crushed with a wooden spoon and placed in 5-liter glass containers. To increase the surface area of a substance, it is necessary to break it into small pieces. The surface-to-volume ratio for the same substance increases as the substances become smaller. Therefore, fruits are cut into small pieces to increase the surface area on which acetic acid bacteria (mostly Acetobacter) will react. Then, in order to kill the microorganisms, 2 liters of spring water, which was first boiled and then cooled, was added to the glass containers.

For the fermentation processes to take place efficiently, 1 liter space was left in the glass containers and their mouths were tightly closed. For the formation of anaerobic fermentation, which is the first of the fermentation processes, the tightly closed glass containers were kept in a dark place for about 3 months at room temperature (RT). Then, it was concluded that the ethanol fermentation took place in a healthy way, since all the fruits sank to the bottom of the glass containers. Then, to start the aerobic fermentation, which is the second fermentation process, firstly the fruit residues were filtered from the glass containers. In order to accelerate the acetic acid fermentation, we added 0.25 liters of vinegar, which we obtained earlier from the same type of fruit with the same technique, to each glass container. The containers were covered with

thin cloths to allow oxygen flow and the acetic acid fermentation was started at RT in the dark environment. After about six months in total, the 1st and 2nd fermentation processes were completed and we produced traditional homemade apple, grape and hawthorn vinegars.

For the production of the blended apple, grape and hawthorn vinegars, we carried out the same processes that we used in the production of the previous pure vinegars in the first stages. Differently, before starting all fermentation processes, ten chickpeas, a teaspoon of cracked wheat and a tablespoon of granulated sugar were added to each glass container to increase the glucose rate. In this method, ethanol fermentation, which is the first fermentation process, took place one month earlier compared to pure vinegars. After about 5 months, all fermentation processes were completed and we produced the blended apple, grape and hawthorn traditional homemade vinegars.

B. Spectroscopy and Rheology Measurements

The dielectric measurements were conducted within a frequency range of 100 Hz to 1 MHz using an Fytronix Dielectric Measurement System at RT. In dielectric measurements, deionized water was used as the baseline, and then 6% aqueous solutions of vinegar were prepared and real and imaginary values of the complex dielectric constant were measured. Based on these measured values, the system created data by calculating the real and imaginary parts of the complex impedance for all samples using its own internal software. Using the real and imaginary parts of the complex impedance, plane plots corresponding to the equivalent impedance circuit on the Smith chart were created.

The UV-vis spectra for the apple, blended apple, grape, blended grape, hawthorn and blended hawthorn vinegars were obtained in the wavelength range of 190 nm to 600 nm by using A 360 Spectrophotometer (AOE Instruments). The optical band gaps (E_g) for all samples were calculated by using the UV-vis spectra. During the experiments, the deionized water which in the quartz cuvette of the UV-vis spectrophotometer was used as baseline for the absorbance spectra in the selected wavelength range. The rectangular quartz cuvette with a volume of 3.5 mL was filled with a mixture of vinegar and deionized water containing 6% vinegar.

Molecular characteristics for all samples, The FTIR analysis were made using Bruker Vertex 70 Fourier transform infrared spectrometer. The FTIR analysis of the vinegars were performed in the wavenumbers range of 4200 to 400 cm⁻¹ with 1 cm/s scanning speed and 4 cm⁻¹ resolution at RT.

The rheological measurements for all samples were performed using a rheometer (Malvern Kinexus Pro.). To perform rheological measurements, shear stress values for all samples were measured from a steady state shear rate starting from a single point and changing step by step. The viscosity values for all samples were obtained as the ratio between steady-state shear stress and shear rate. Besides, the frequency evolution of the storage and loss modulus for the apple, blended apple, grape, blended grape, hawthorn and hawthorn blended vinegars were recorded in the frequency range of 10^{-2} to 10^{3} rad/s.

C. Theory

C. 1. Dielectric

The energy stored and lost within the material is defined by the dielectric constant, which is a complex quantity (Macdonald, 1992; Okutan et al., 2024)

$$\varepsilon^*(\omega) = \varepsilon'(\omega) - j\varepsilon''(\omega). \tag{1}$$

In the equation, $\varepsilon'(\omega)$ and $\varepsilon''(\omega)$ are the real and imaginary parts of the complex dielectric constant, describing the energies stored and lost within the material, respectively. Also, j is the imaginary factor; ($j = \sqrt{-1}$), $\omega = 2\pi f$ the angular frequency.

The tangent factor or loss factor was given using the following relation

$$tan\delta = \varepsilon''(\omega)/\varepsilon'(\omega). \tag{2}$$

Impedance, which is a complex quantity, is defined as in the equation below. In the equation, $Z'(\omega)$ and $Z''(\omega)$ are the real and imaginary parts of the complex impedance, which define the resistance and reactance, respectively (Mazzer et al., 2018)

$$Z^*(\omega) = Z'(\omega) + jZ''(\omega). \tag{3}$$

The equation describing the Cole-Cole relaxation model for the complex impedance includes three components (Elwakil & Maundy, 2010; Coşkun et al., 2019; Cole & Cole, 1941).

$$Z^*(\omega) = R_{\infty} + \frac{R_0 - R_{\infty}}{1 + (i\omega\tau^{\alpha})}.$$
 (4)

These components in the equation are R_0 , R_∞ , and α , which define a low-frequency resistor, a high-frequency resistor, and a constant phase factor, respectively. $Z_{CPE} = 1/(i\omega C)^{\alpha}$ defines the impedance of the constant phase element. Here, $(i\omega)^{\alpha} = \omega^{\alpha} \left[\cos\left(\frac{\alpha\pi}{2}\right) + i\sin\left(\frac{\alpha\pi}{2}\right)\right]$ and C is the capacitance. The α changes from zero to one $(0<\alpha\leq 1)$.

C. 2. Optic

One of the most important laws in the optical spectroscopy, the Beer-Bouguer-Lambert law given below (Di Capua et al., 2014; Owen, 1996; Mach, 2003; Bouguer, 1760; Lambert, 1760; Beer, 1852), was used to interpret the UV-vis absorption spectra of the samples,

$$A = -\log(T) = \log(I_0/I) = \varepsilon l c.$$
(5)

Here, A, T, I, I0, ε , I and C0 correspond to the absorbance, transmittance, transmitted intensity, incident intensity, extinction coefficient, light path length and concentration of the material was used, respectively. The Beer-Bouguer-Lambert law states that the amount of light absorbed is proportional to the number of absorbing molecules through which the light passes.

The optical band gaps (E_g) contributes to our understanding of the electrical behavior of a material. The E_g of materials can be found by using Tauc model (Tauc, 1968; Chand et al., 2017). The E_g values of the vinegars are found by the following equation

$$\alpha h \nu = B(h \nu - E_g)^n. \tag{6}$$

Where, α , h, ν , B, E_g and n refer to the absorption coefficient, Planck's constant, the frequency of the incident photon, a constant that depends on the transition probability, energy band gap and the index related to the transition, respectively.

C. 3. Rheology

Fluids show two types of flow behavior as Newtonian and non-Newtonian. Fluids in which the shear rate at any point is determined only by the value of the shear stress at that point are known as Newtonian fluids. Viscosity is the most important flow parameter showing the measure of resistance to fluid flow under an applied force. The viscosity of Newtonian fluids depend on the shear stress and shear rate and is calculated by the following equation (Doolittle, 1951; Batchelor, 1967; Falcone et al., 2027)

$$\eta = \tau/\dot{\gamma}.\tag{7}$$

Where, η , τ and $\dot{\gamma}$ refer to viscosity, shear stress and shear rate respectively. The non-Newtonian flow behaviour of fluid flow is explained by the Ostwald-de Waele model (or power law) given by (Chhabra & Richardson, 1999; Nguyen & Nguyen, 2012)

$$\eta = K(\dot{\gamma})^{m-1}. \tag{8}$$

In the equation, K is the fluid consistency coefficient and m is the flow behaviour index, respectively. According to this model, m < 1 corresponds to non-Newtonian shear-thinning fluid behavior, m > 1

corresponds to non-Newtonian shear-thickening fluid behavior and m = 1 corresponds to the standard Newtonian fluid behavior.

The viscoelastic behaviour of the flow properties of fluids are determined by the complex modulus given by

$$G^* = \sqrt{(G')^2 + (G'')^2}. (9)$$

Here, G' is elastic modulus and G'' is viscous given in the equation define the storage and loss modulus, respectively. Moreover, the complex viscosity is calculated in the following equation

$$\eta^* = G^* / \omega = \sqrt{(G')^2 + (G'')^2} / \omega \,, \tag{10}$$

here, η^* , G^* and ω are the complex viscosity, complex modulus and oscillation frequency, respectively (Öztürk et al., 2022; Gunasekaran & Ak, 2000; Dogan et al., 2013; Laun et al., 2014).

III. RESULTS AND DISCUSSION

Frequency variation of the real $(\varepsilon'(f))$ and imaginary $(\varepsilon''(f))$ parts of the complex dielectric constant $(\varepsilon^*(f))$ for the apple, blended apple, grape, blended grape, hawthorn, blended hawthorn vinegars was shown in Figures 1a and b, respectively. The tangent factor (tanδ), which reveals whether there are dielectric relaxations in the material in the frequency range of 10^2 Hz to 10^6 Hz is given in Figure 1c. It was determined that the dielectric parameters ($\varepsilon'(f)$ and $\varepsilon''(f)$) of all vinegars tend to gradually decrease with increasing frequency, consistent with the behavior of a dielectric material. It was observed that all vinegars had the highest dielectric values in the low frequency region due to the electrode polarization caused by the alignment of the free ions of organic acids and phenolic compounds in the direction of the applied external electric field (Yalçın et al., 2021; Öztürk et al., 2022; Lambert, 1760). A significant contribution to the high dielectric values of the vinegars in this region comes from the Maxwell-Wagner interfacial polarization effect created by the free charges of the samples between two electrodes to which an electric field is applied (Vu et al., 2017; Jana et al., 2007; Wagner, 1914). The fact that the highest and lowest dielectric values in the low frequency region belong to grape and blended apple vinegars, respectively, is due to the different organic acid and phenolic compound concentrations that affect the polarization mechanisms of these vinegars. The dielectric values for all samples decreased almost exponentially because the free ions in the structure of the vinegar could not find the necessary time to orient themselves in the direction of the external electric field applied with increasing frequency. In the high frequency region, the electrode and interface polarization effects on the dielectic parameters of the vinegars lose their effectiveness and the samples are now under the effect of dielectric relaxation in this region. When the $tan\delta$ graph, which gives an important idea about the dielectric relaxation processes of the samples, is analyzed, it is clearly seen that the vinegars tend to have a peak value (Mazzer et al., 2018; Ali et al., 2022; Fernandes et al., 2017; El Khaled et al., 2016; Routraya & Orsat, 2014). The fact that the $tan\delta$ value of the samples have peak values was interpreted as a sign that a dielectric relaxation process was experienced and therefore Cole-Cole plots could form (Cole & Cole, 1941).

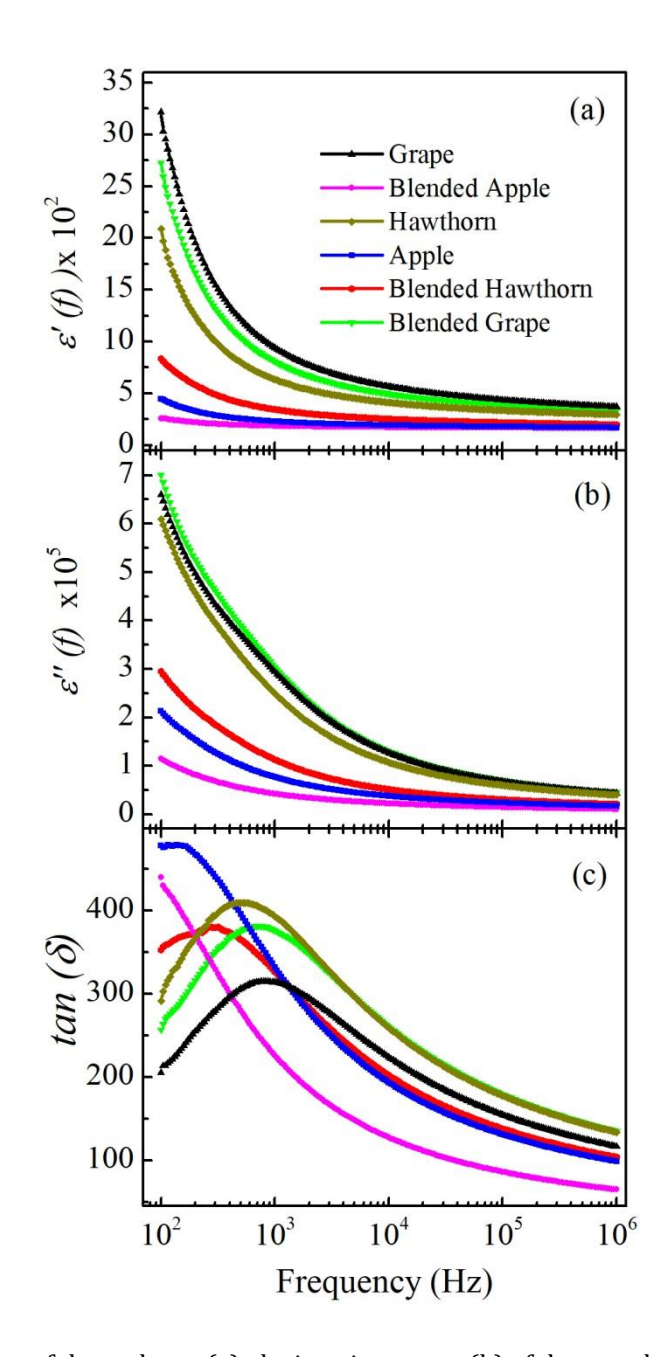


Figure 1. Frequency evolution of the real part (a), the imaginary part (b) of the complex dielectric constant and the tangent factor (c) for all vinegars.

Figure 2 shows the evolution of the complex impedance for the apple, blended apple, grape, blended grape, hawthorn and blended hawthorn vinegars in the frequency range of 10^2 Hz to 10^6 Hz. It was observed that the impedance evolution of all vinegars in the low frequency region was independent of frequency. Each vinegar has its highest impedance value in the region below the 10^5 Hz frequency. The electrode and interface polarization mechanisms experienced in this region provide an internal resistance against the free charges inherent in all vinegars moving in the direction of the applied field. The high impedance values were recorded in all samples in the frequency region below 10^5 Hz due to the internal resistance against this free charge flow. The impedance values of all samples work inversely with the $\varepsilon'(f)$, where the results of electrode polarization effects are best seen (Ali et al., 2022; Fernandes et al., 2017; El Khaled et al., 2016; Routraya & Orsat, 2014; Okutan et al., 2023). The fact that depending on the concentration of free charge carriers in the vinegars, the highest impedance value belong to blended apple vinegar. In the high frequency region, the impedance values of all vinegars are under the influence of the dielectric relaxation process. The impedance values of all samples decrease as the free charge carriers of phenolic compounds and organic acids can move in the direction of the field without encountering any internal resistance due to the dielectric

relaxation experienced in this region (Öztürk et al., 2022; Macdonald, 1992; Coşkun et al., 2019; Wang et al., 2019; Bao et al., 1992; Okutan et al., 2021). At the end of the dielectric relaxation process, the impedance of all vinegars goes towards almost the same value.

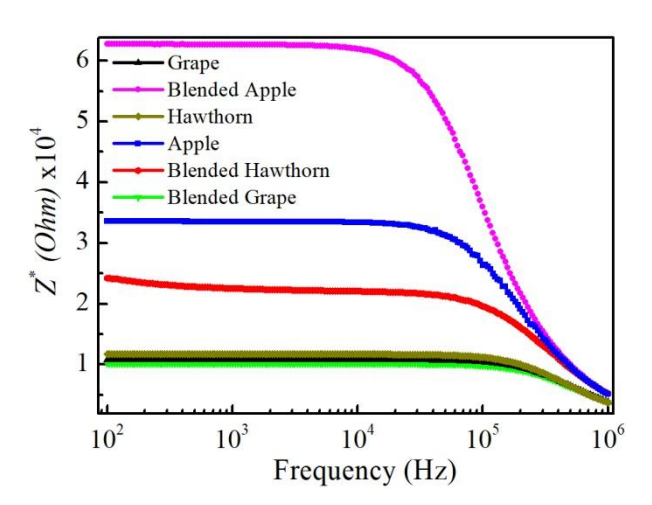


Figure 2. Frequency evolution of the complex impedance for all vinegars.

Experimental data formed by plane plots of the real (Z'(f)) and imaginary (Z''(f)) parts of the complex impedance (Z^*) of vinegars on the Smith chart are shown in Figure 3. It was observed that the complex impedance plane (Z'-Z'') plots of all the vinegars tended to form a semicircle (Coşkun et al., 2019; Ali et al., 2022; Padmamalini & Ambujam, 2016). While these plane plots are tend to form a complete semicircle in the high frequency region for all vinegars, which is compatible with the Debye model (Debye, 1929), it is seen that they cannot complete the semicircle due to the strong polarization experienced at low frequencies. In this case, the dielectric relaxation mechanism that enables the formation of the Z'-Z'' plots can be explained by the Cole-Cole relaxation model for all examples (Cole & Cole, 1941). In fact that these Cole-Cole plots on the Smith chart correspond to an impedance circuit (Smith, 1939; Malisuwan & Sivaraks, 2013; Okutan et al., 2023; Görgülüer et al., 2024). This equivalent impedance circuit for vinegars consists of capacitance and resistance connected in series. The relevant circuit is given schematically in Figure 3. These Cole-Cole plots on the Smith chart, which are formed as a result of the dielectric relaxation process, actually offer important inferences in determining the conductivity of vinegars. So, it can be predicted that the conductivity of blended apple vinegar, represented by the large semi-circle, will be higher than the others. This high conductivity is originated from the concentration of organic acids and phenolic compounds containing free charge carriers in the structure of this sample. Therefore, quantum mechanical tunneling, which is the wave nature of particles, implies that a particle can pass through the potential energy barrier even if there is not enough energy to overcome this tunnel. In this context, the concentration of organic acids and phenolic compounds, which are the most important parameters in determining the quality of vinegars, can be determined by the size of the semicircles on the Smith chart, which has extremely meaningful results. In addition, these results provide important information that vinegar can be used as an equivalent electronic circuit element (Öztürk, 2021a, 2021b; Yalçın et al., 2021; Öztürk et al., 2022; Okutan et al., 2024; Coskun et al., 2019).

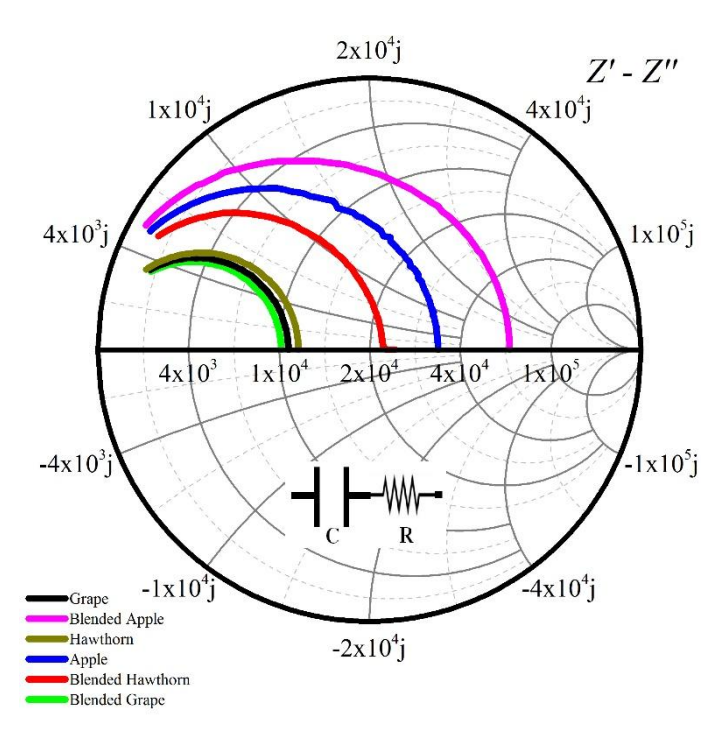


Figure 3. Smith chart for the complex impedance planes of all vinegars and their equivalent impedance circuit.

Wavelength evolution of the UV-vis absorption spectra spectra for the apple, blended apple, grape, blended grape, hawthorn and blended hawthorn vinegars in the wavelength range of 190 to 600 nm are shown in Figure 4. It is seen that the UV-vis spectra for all vinegars have two peaks in the wavelength range of 190 to 300 nm. The main peak of the UV-vis spectra of vinegars in the wavelength range of 190 to 240 nm is due to the organic acids (mostly acetic acid), which allows the characterization, identity and authenticity of the vinegars to be verified (Entani et al., 1998; Liu et al., 2019; Öztürk, 2021a, 2021b; Yalcın et al., 2021; Lynch et al., 2019; Beisl et al., 2018). In this wavelength region, the strongest peak values were obtained for blended hawthorn, apple and blended apple vinegars, respectively. The peak values of vinegars in the wavelength range of 250 to 300 nm were attributed to the presence of phenolic compounds that give antioxidant properties to vinegars (Liu et al., 2019; Aleixandre-Tudo & du Toit, 2019; García-Parrilla et al., 1994). In this wavelength region, the strongest peak values belong to blended apple, apple and blended hawthorn vinegars, respectively. Based on this result, it was concluded that the blended vinegars have more phenolic compounds than the pure vinegars. Furthermore, it was concluded that the reason for the shifts in the positions of the two main peaks in the UV-vis spectra of pure and blended vinegars is due to the molecular structures of organic acids and color pigments. According to all results, it was concluded that UVvis absorption spectroscopy analysis can contribute to the solution of food spectral trace authentication and quality control problems for vinegar and similar fluid.

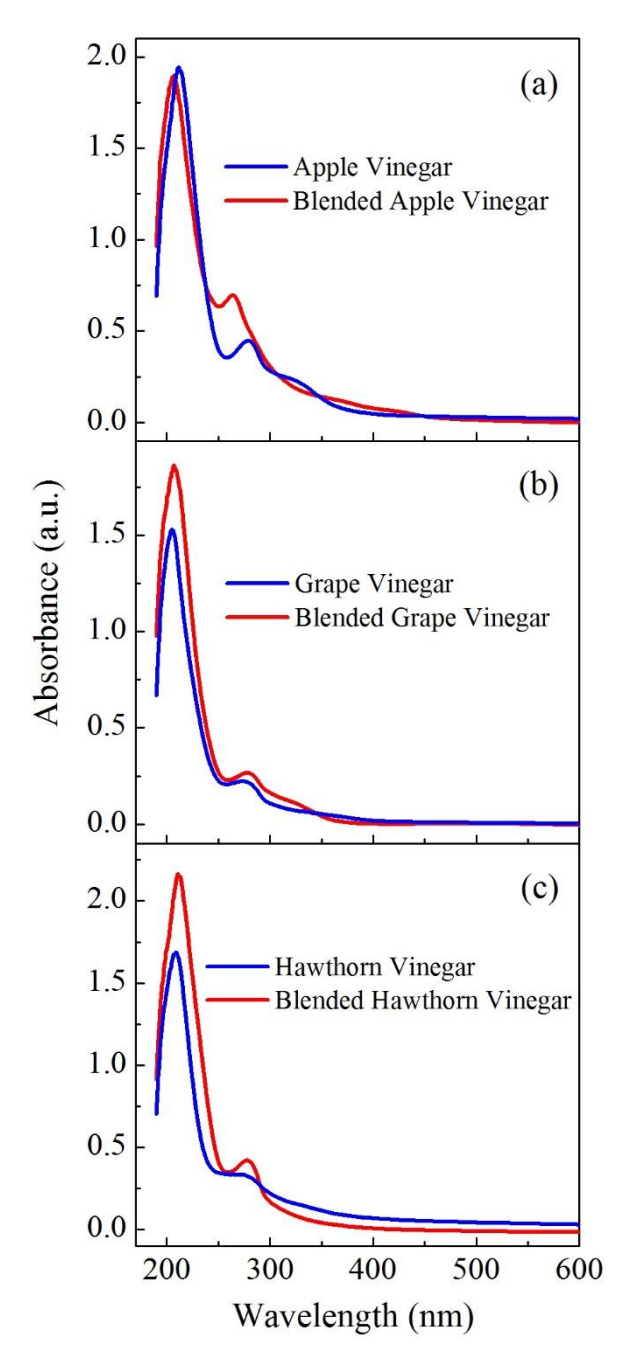


Figure 4. UV-vis spectra for apple and blended apple (a), grape and blended grape (b), hawthorn and blended hawthorn (c) vinegars.

Energy (hv) evolution of the $(\alpha hv)^2$ for all the vinegars in the energy range of 2.5 to 6.5 eV are shown in Figure 5. The dashed lines in this Figure show the tangent and are used to obtain the optical band gaps (E_g) (Tauc, 1968; Chand et al., 2017). From this graph, it can be seen that vinegar molecules do not undergo significant interactions with photons with energy lower than about 5.21 eV. It was concluded that the peaks formed after the energy value of about 5 eV with the increasing photon energy were caused by organic acid concentration and phenolic compounds. It is clearly seen that the E_g values don't show a dependence on energy that below the energy value of about 5.21 eV. In other words, it was attributed that the substances found in vinegar being subject to the quantum confinement property such as phenolic compounds and melanoidins were mainly effective on the E_g values in the high energy region. The shifts in the positions of the peaks in the spectra were attributed to the widening of the optical energy band gap caused by the quantum confinement effect originating from the organic acids in the vinegar structure. As seen in Figure 5, the E_g values for apple and blended apple (Figure 5a), grape and blended grape (Figure 5b), hawthorn and

blended hawthorn (Figure 5c) vinegars were found as 5.21 eV, 5.28 eV, 5.36 eV, 5.38 eV, 5.41 eV and 5.26 eV, respectively. If we compare the blended and pure vinegars over all the energy gaps we found, although the E_g values of blended apple and apple vinegars was the same, but for other types of vinegars the E_g values of the blended vinegars are much lower than pure vinegars. As a result, we obtained the result that the blended grape and blended hawthorn vinegars contain more phenolic compounds than the pure types, but they can react with the light which has lower energy. Thus, the UV-vis spectroscopy technique has been shown to be one of the most economical and simplest spectroscopic techniques applied to vinegars, based on measuring the absorption of electromagnetic radiation by molecules (Singh et al., 2015; Jeans, 1905; Rayleigh, 1900; Caron-Decloquement, 2010). This property is attributed to the photon energy quantize structure. The relationship between the quantum confinement effect and photon energy can be seen in Figure 6.

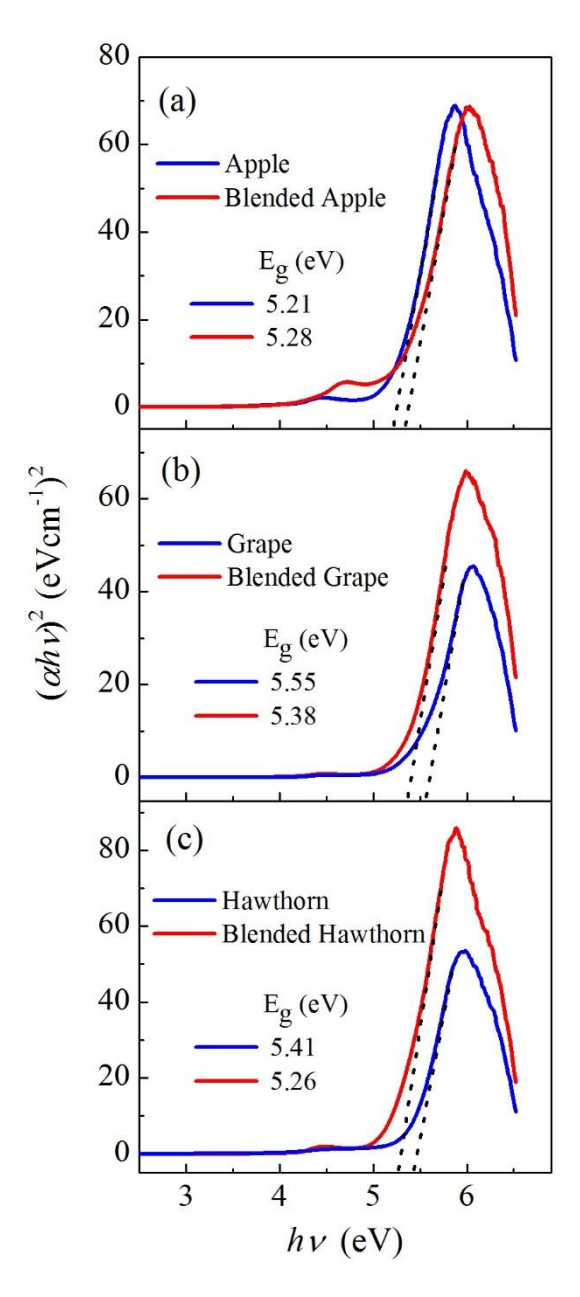


Figure 5. Energy evolution of $(\alpha h \nu)^2$ for apple and blended apple (a), grape and blended grape (b), hawthorn and blended hawthorn (c) vinegars.

The wavelength evolution of the experimental and theoretical photon energy is given in Figure 6. The photon energy range from violet to red in the visible light region is 3.26 to 1.63 eV, respectively. These energies are at the level between the outer electron shells of the organic acid molecules in vinegar. The

quantum confinement effect occurs when the particle size of the structures inside organic acid molecules is too small to be compared with the wavelength of the electron. In order to reach the minimum Eg value in vinegar, it is necessary to exceed the photon energy value of 3.26 eV. In this case, the energy levels in the area within the molecular shell are defined with an energy above the visible region, and the minimum Eg value was recorded as 5.21 eV in this study.

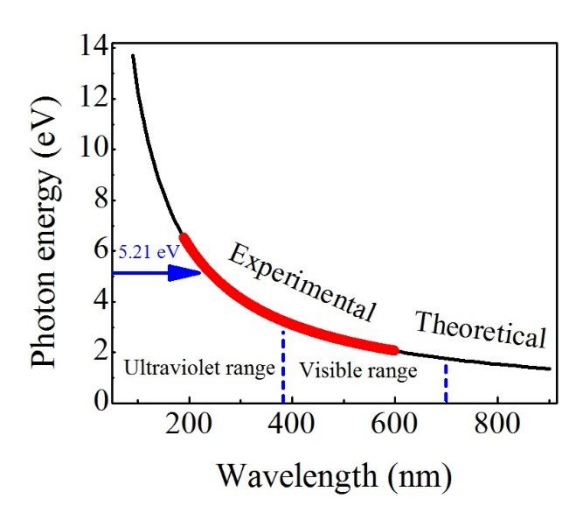


Figure 6. Wavelength evolution of the experimental and theoretical photon energy.

The wavenumbers dependence of absorbance for apple, blended apple, grape, blended grape, hawthorn and blended hawthorn vinegars in the wavenumber range of 4200 cm⁻¹ to 400 cm⁻¹ were shown in Figures 7a, b, c, d, e and f, respectively. The spectral peaks for all samples showed similar characteristics, although there are minor differences in the region of 1300 cm-1. It was seen that the FTIR spectra for apple, blended apple, grape, blended grape, hawthorn and blended hawthorn vinegars have two distinct peaks corresponding to wavenumbers of around 3300 and 1635 cm⁻¹. It was observed that the peaks of the spectral peaks corresponding to wavenumber of around 3300 cm⁻¹ originate from the stretching vibrations of hydrogen-bonded OH groups in phenolic and aliphatic structures of all vinegars (Öztürk, 2021a; Caron-Decloquement, 2010; Williams & Fleming, 1989; Feng et al., 2016; Yalçın et al., 2022; Liu et al., 2011; Ríos-Reina et al., 2017; Kadiroğlu, 2018). The peaks in the same region in the FTIR spectra of blended apple, blended grape, and blended hawthorn vinegars shifted to lower wavenumbers compared to apple, grape and hawthorn vinegars. It was determined that the shifting in this region is due to the blending property of blended apple, blended grape, and blended hawthorn vinegars. The peaks around 1635 cm⁻¹ in the spectra are the result of the H-O-H stretching vibrations and the aromatic C=C stretching vibrations from organic acids and phenolic compounds in traditional homemade vinegars (Öztürk, 2021a; Caron-Decloquement, 2010; Williams & Fleming, 1989; Feng et al., 2016; Yalcın et al., 2022; Liu et al., 2011; Ríos-Reina et al., 2017; Kadiroğlu, 2018). The H-O-H molecule vibrates when it absorbs vibrational energy equal to the frequency of the photon. As a result, it is possible to say that even small changes in the positions of these two distinct peaks affect the quality of vinegars.

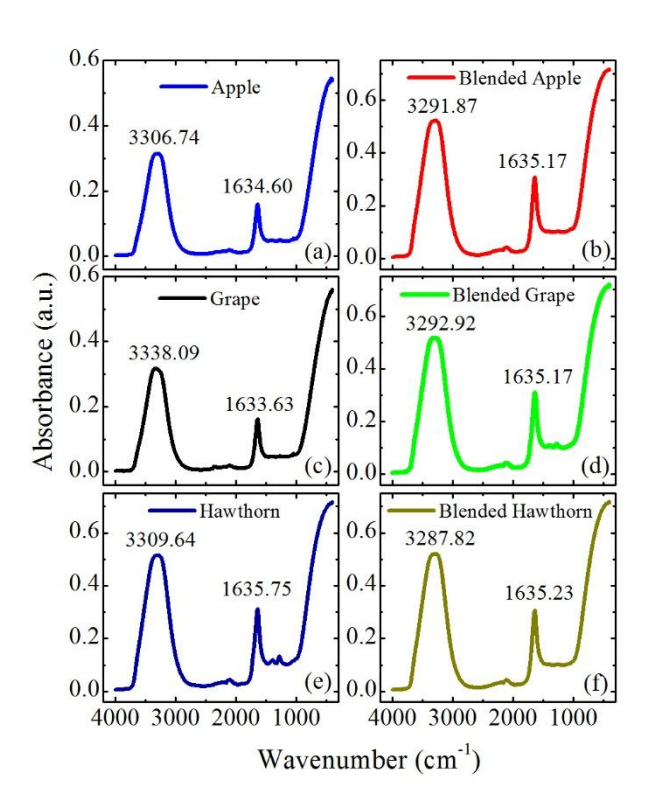


Figure 7. FTIR spectra for the apple, blended apple, grape, blended grape, hawthorn and blended hawthorn vinegars.

Shear rate evolution of the viscosity for all samples in the shear rate range of $0 \, s^{-1}$ to $4 \, s^{-1}$ were shown in Figure 8. It is seen that the viscosity curves for all vinegars exhibit very similar behavior in shear rate range of $0 \, s^{-1}$ to $1.5 \, s^{-1}$. In the region where the shear rate value is bigger than $3 \, s^{-1}$, the viscosity values of apple, blended apple, grape, blended grape, hawthorn vinegars increased rapidly, while the viscosity value of blended hawthorn vinegar did not increase as much as the others. Again, as can be seen from the viscosity graphs, apple, blended apple, grape, blended grape, hawthorn and blended hawthorn vinegars show non-Newtonian shear-thickening (dilatant) fluid behavior (Chhabra & Richardson, 1999; Nguyen & Nguyen, 2012; Kassim & Sarow, 2020).

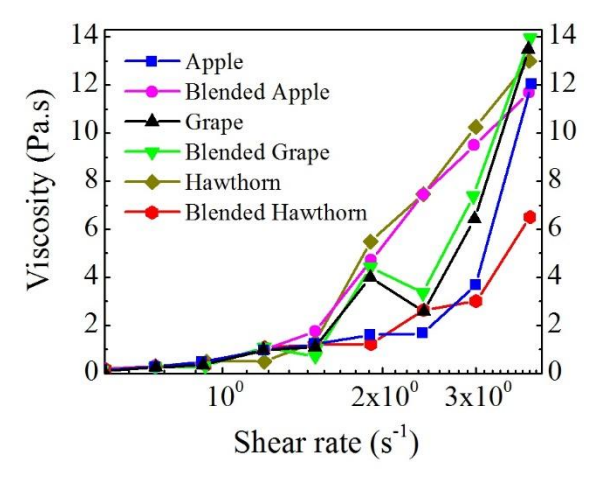


Figure 8. Shear rate evolution of viscosity for apple, blended apple, grape, blended grape, hawthorn and blended hawthorn vinegars.

Frequency evolution of the reel (storage modulus) and imaginary (loss modulus) parts of complex modulus for the apple, blended apple, grape, blended grape, hawthorn and blended hawthorn vinegars have showed in Figures 9a and b, respectively.

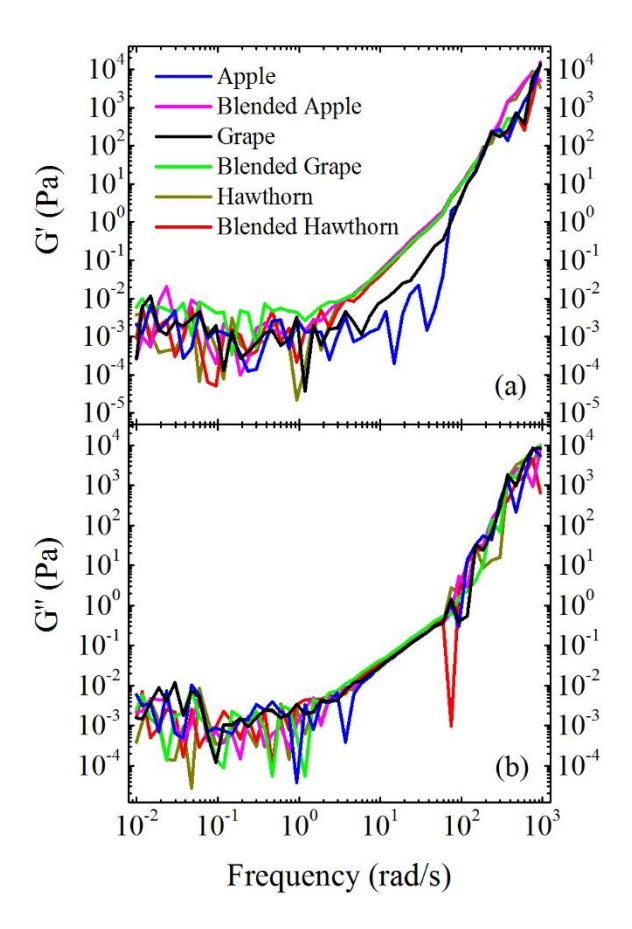


Figure 9. Frequency evolution of the storage (a) and loss (b) modulus for apple, blended apple, grape, blended grape, hawthorn and blended hawthorn vinegars.

As seen in Figure 9, frequency evolution of the storage (G') and loss (G'') modules for all vinegars are very similar and increase almost exponentially with increasing frequency after 1 rad/s. The G' and G'' modulus curves, which refer to the elastic and viscous behaviors of the apple, blended apple, grape, blended grape, hawthorn and blended hawthorn vinegars, show non-Newtonian flow properties in accordance with the Power Law (Chhabra & Richardson, 1999; Nguyen & Nguyen, 2012; Gunasekaran & Ak, 2000; Dogan et al., 2013). Furthermore, it was observed in Figure 9. that the viscous behaviour of the loss modules values for all vinegars was more stable while the storage values was unstable in the frequency range of 10^1 to 10^2 rad/s.

IV. CONCLUSION

In this study, the impedance spectroscopy, ultraviolet-visible spectroscopy, Fourier transform infrared spectroscopy and rheology techniques were used for quality control, characterization and authentication of the apple, blended apple, grape, blended grape, hawthorn and blended hawthorn traditional homemade vinegars. The frequency evolution of dielectric parameters for all vinegars was characterized in the frequency range from 100 Hz to 1 MHz at RT. The effects of polarization mechanisms on the dielectric properties of the samples in the low and high frequency regions were analyzed and the compatibility of all vinegars with Maxwell-Wagner theory and relaxation models was revealed. The highest and lowest dielectric values determined by electrode and interface polarizations were recorded for grape and blended apple vinegars, respectively. In fact, the low or high dielectric values of vinegars are a result of the concentration of organic acids and phenolic compounds in their structures that determine their quality. It was seen that the relaxation of the complex impedance plane plots of the vinegars was compatible with the

Cole-Cole model and these plots corresponded to the impedance circuit in the Smith chart. The fact that the largest semicircle on the Smith chart belongs to blended apple vinegar was attributed to its higher conductivity than the others. The UV-vis spectra of all vinegars were found to have two peaks in the wavelength range of 190 to 300 nm. The main peak of the UV-vis spectra of vinegars in the wavelength range of 190 to 240 nm was determined to originate from organic acids, which allowed the characterization of the vinegars to be verified as to their identity and authenticity. In this wavelength region, the strongest peak values were obtained for blended hawthorn, apple, and blended apple vinegars, respectively. The peak values in the UV-vis spectra in the wavelength region of 250 nm to 300 nm were attributed to phenolic compounds that give antioxidant properties to vinegars. It was determined that the strongest peak values in this wavelength region belonged to blended vinegars, respectively, According to this result, it was concluded that the blended vinegars have more phenolic compounds than the pure vinegars. The optical band gap values for the apple and blended apple, grape and blended grape, hawthorn and blended hawthorn were recorded as 5.21 eV, 5.28 eV, 5.55 eV, 5.38 eV, 5.41 eV and 5.26 eV, respectively. If we compare the blended and pure vinegars in terms of optical band gaps we found, the $\it E_{\it g}$ values of most blended vinegars are much lower than those of the pure vinegars. We concluded that the blended grape and blended hawthorn vinegars contain more phenolic compounds than the pure types, but they can react with the light which has lower energy. It was concluded that in order to reach the minimum Eg value in homemade vinegars, the band gap energy value of 5.21 eV must be exceeded.

FTIR spectra for the apple, blended apple, grape, blended grape, hawthorn and blended hawthorn vinegars have two distinct peaks corresponding to wavenumbers of around 3300 cm⁻¹ and 1635 cm⁻¹. It was concluded that the peaks of the spectral peaks corresponding to wavenumber of around 3300 cm⁻¹ are originating from stretching vibration of hydrogen bonded OH groups in phenolic and aliphatic structures of all vinegars. The peaks corresponding to wavenumber of around 3300 cm⁻¹ in the FTIR spectra of blended apple, blended grape, and blended hawthorn vinegars shifted to lower wavenumbers compared to apple, grape and hawthorn vinegars. It has been clearly determined that the shifting in this region is due to the blending property of blended apple, blended grape, and blended hawthorn vinegars. The peaks around 1635 cm⁻¹ in the spectra are the result of the H-O-H stretching vibrations and the aromatic C=C stretching vibrations from organic acids and phenolic compounds in traditional homemade vinegars. From the flow behaviors and viscosity curves of apple, blended apple, grape, blended grape, hawthorn and blended hawthorn vinegars, it was revealed that all vinegars have non-Newtonian shear-thickening (dilatant) fluid behavior.

DECLARATIONS

Acknowledgements: This work was financially supported by Scientific Research Projects Coordination Unit of Niğde Ömer Halisdemir University with Project No.: FMT 2022/1-LÜTEP

Author Contributions: O.Y.; Sample production and preparation, Writing – review & editing, M.Ö.; Investigation, Writing–review & editing, Ö.G.; Investigation, Conceptualization, Sample preparation, Writing – review & editing, M.A.; Investigation, Sample production and preparation.

Conflict of Interest Disclosure: The authors declare that they have no conflict of interest.

Copyright Statement: The authors retain the copyright of their work published in the journal, which is licensed under the CC BY-NC 4.0 license, allowing others to share and adapt the work for non-commercial purposes with appropriate attribution.

Funding/Supporting Organizations: This research received no external funding.

Ethical Approval and Participant Consent: This study does not involve human or animal participants. All procedures followed scientific and ethical principles, and all referenced studies are appropriately cited.

Plagiarism Statement: This article has been evaluated for plagiarism and no instances of plagiarism were detected.

Availability of Data and Materials: Data sharing is not applicable to this study.

Use of AI Tools: The authors declare that no Artificial Intelligence (AI) tools were used in the creation of this article.

V. REFERENCES

- Adams, M. R. (1998). Microbiology of fermented foods: Vinegar. In *Microbiology of fermented foods* (pp. 1–44). Springer. http://doi.org/10.1007/978-1-4613-0309-1_1
- Aleixandre-Tudo, J. L., & du Toit, W. (2019). The role of UV-visible spectroscopy for phenolic compounds quantification in winemaking. *IntechOpen*. https://doi.org/10.5772/intechopen.79550
- Ali, A., Alabbosh, K. F. S., Naveed, A., Uddin, A., Chen, Y., Aziz, T., Moradian, J. M., Imran, M., Yin, L., Hassan, M., Qureshi, W. A., Ullah, M. W., Fan, Z., & Guo, L. (2022). Evaluation of the dielectric and insulating properties of newly synthesized ethylene/1-hexene/4-vinylcyclohexene terpolymers. *ACS Omega*, 7(35), 31509–31519. https://doi.org/10.1021/acsomega.2c04123
- Bao, J. Z., Davis, C. C., & Schmukler, R. E. (1992). Frequency domain impedance measurements of erythrocytes. Constant phase angle impedance characteristics and a phase transition. *Biophysical Journal*, *61*, 1427–1434. https://doi.org/10.1016/S0006-3495(92)81948-3
- Batchelor, G. K. (1967). *An Introduction to Fluid Dynamics* (Cambridge Mathematical Library series). Cambridge University Press.
- Beer, A. (1852). Bestimmung der Absorption des rothen Lichts in farbigen Flüssigkeiten. *Annalen der Physik*, *162*, 78–88. https://doi.org/10.1002/andp.18521620505
- Beisl, S., Binder, M., Varmuza, K., Miltner, A., & Friedl, A. (2018). UV-Vis spectroscopy and chemometrics for the monitoring of organosolv pretreatments. *Chemical Engineering Transactions*, *2*(4), Article 45. https://doi.org/10.3390/chemengineering2040045
- Bottéro, J. (2004). *The oldest cuisine in the world: Cooking in Mesopotamia*. University of Chicago Press.
- Bouguer, P. (1760). *Traité d'optique sur la gradation de la lumière.* Guerin and Delatour.
- Bourgeois, J. F., & Barja, F. (2009). The history of vinegar and of its acetification systems. *Archives des sciences*, *62*, 147-160. http://doi.org/10.5169/seals-738455
- Budak, N. H., Aykin, E., Seydim, A. C., Greene, A. K., & Guzel-Seydim, Z. B. (2014). Functional properties of vinegar. *Journal of Food Science*, 79, 757–764. https://doi.org/10.1111/1750-3841.12434
- Caron-Decloquement, A. (2010). *Extractives from sitka spruce*. [Doctoral dissertation, University of Glasgow].
- Chand, P., Vaish, S. & Kumar, P. (2017). Structural, optical and dielectric properties of transition metal $(MFe_2O_4; M=Co, Ni and Zn)$ nanoferrites. *Physica B*, 524, 53–63. https://doi.org/10.1016/j.physb.2017.08.060
- Chen, H., Chen, T., Giudici, P., & Chen, F. (2016). Vinegar functions on health: constituents, sources, and formation mechanisms. *Comprehensive Reviews in Food Science and Food Safety*, *15*, 1124–1138. https://doi.org/10.1111/1541-4337.12228
- Cheng, Z., Ran, Q., Liu, J., Deng, X., Qiu, H., Jia, Z., & Su, X. (2020). Rapid determination for benzoic acid, sorbic acid, phenyllactic acid, phenylalanine, and saccharin sodium in vinegar by high-performance liquid chromatography–UV. *Food Analytical Methods*, *13*, 1673–1680. https://doi.org/10.1007/s12161-020-01784-6
- Chhabra, R. P., & Richardson, J. F. (1999). *Non-Newtonian flow and applied rheology: Engineering applications*. Butterworth-Heinemann. https://doi.org/10.1016/B978-0-7506-8532-0.X0001-7
- Cole, K. S., & Cole, R. H. (1941). Dispersion and absorption in dielectrics I. Alternating current characteristics. *The Journal of Chemical Physics*, *9*, 341–351. https://doi.org/10.1063/1.1750906
- Coşkun, R., Okutan, M., Öztürk, M., & Yalçın, O. (2019). Experimental model to describe the dielectric response of different dye and nanoparticles doped hydrogels for biological cell membranes and biological systems. *Journal of Molecular Liquids*, 296, Article 112072. https://doi.org/10.1016/j.molliq.2019.112072
- de Oliveira, S. R., & Neto, J. A. G. (2007). Evaluation of Bi as internal standard to minimize matrix effects on the direct determination of Pb in vinegar by graphite furnace atomic absorption spectrometry using Ru permanent modifier with co-injection of Pd/Mg(NO₃)₂. Spectrochimica Acta Part B: Atomic Spectroscopy, 62, 1046–1050. https://doi.org/10.1016/j.sab.2007.06.007
- Debye, P. (1929). Polar molecules. The Chemical Catalog Company Inc.
- Di Capua, R., Offi, F., & Fontana, F. (2014). Check the Lambert–Beer–Bouguer law: A simple trick to boost the confidence of students toward both exponential laws and the discrete approach to experimental physics. *European Journal of Physics*, *35*, Article 045025. https://doi.org/10.1088/0143-0807/35/4/045025
- Dogan, M., Kayacier, A., Toker, Ö. S., Yilmaz, M. T., & Karaman, S. (2013). Steady, dynamic, creep, and recovery analysis of ice cream mixes added with different concentrations of xanthan gum. *Food and Bioprocess Technology*, *6*, 1420–1433. https://doi.org/10.1007/s11947-012-0872-z
- Doolittle, A. K. (1951). Studies in Newtonian flow. I. The dependence of the viscosity of liquids on temperature. *Journal of Applied Physics*, *22*, 1031-1035. https://doi.org/10.1063/1.1700096

- El Khaled, D., Castellano, N. N., Gázquez, J. A., Perea-Moreno, A. J., & Manzano-Agugliaro, F. (2016). Dielectric spectroscopy in biomaterials: Agrophysics. *Materials*, 9(5), Article 310. https://doi.org/10.3390/ma9050310
- Elwakil, A. S., & Maundy, B. (2010). Extracting the Cole-Cole impedance model parameters without direct impedance measurement. *Electronics Letters*, 46(20), 1367–1368. https://doi.org/10.1049/el.2010.1924
- Entani, E., Asai, M., Tsujihata, S., Tsukamoto, Y., & Ohta, M. (1998). Antibacterial action of vinegar against food-borne pathogenic bacteria including Escherichia coli 0157:H7. *Journal of Food Protection*, 61(8), 953–959. https://doi.org/10.11150/kansenshogakuzasshi1970.71.451
- Falcone, P. M., Chillo, S., Giudici, P. A., & Del Nobile, M. (2007). Measuring rheological properties for applications in quality assessment of traditional balsamic vinegar: Description and preliminary evaluation of a model. *Journal of Food Engineering*, 80(1), 234–240. https://doi.org/10.1016/j.jfoodeng.2006.05.023
- Feng, S., Yuan, Z., Leitch, M., Shui, H., & Xu, C. C. (2016). Effects of bark extraction before liquefaction and liquid oil fractionation after liquefaction on bark-based phenol formaldehyde resoles. *Industrial Crops and Products*, 84, 330–336. https://doi.org/10.1016/j.indcrop.2016.02.022
- Fernandes, P. R. G., da Silva, K. A., Mukai, H., & Muniz, E. C. (2017). Optical, morphological and dielectric characterization of MBBA liquid crystal-doped hydrogels. *Journal of Molecular Liquids*, 229, 319–329. https://doi.org/10.1016/j.molliq.2016.12.080
- García-Parrilla, M. C., Camacho, M. L., Heredia, F. J., & Troncoso, A. M. (1994). Separation and identification of phenolic acids in wine vinegars by HPLC. *Food Chemistry*, *50*, 313–315. https://doi.org/10.1016/0308-8146(94)90140-6
- Görgülüer, Ö., Coşkun, R., Yalçın, O., Okutan, M., Uslu, H., & Doğanay, B. Ş. (2024). Structural, morphological and dielectrical properties of acorn cupule extract doped hydrogels. *Journal of Molecular Structure*, *1309*, 138120. https://doi.org/10.1016/j.molstruc.2024.138120
- Guerrero, E. D., Mejías, R. C., Marín, R. N., Lovillo, M. P., & Barroso, C. G. (2010). A new FT-IR method combined with multivariate analysis for the classification of vinegars from different raw materials and production processes. *Journal of the Science of Food and Agriculture*, *90*, 712–718. https://doi.org/10.1002/jsfa.3873
- Gunasekaran, S., & Ak, M. M. (2000). Dynamic oscillatory shear testing of foods—selected applications. *Trends in Food Science & Technology*, 11, 115–127. https://doi.org/10.1016/S0924-2244(00)00058-3
- Ho, C. W., Lazim, A. M., Fazry, S., Zaki, U. K. H. H., & Lim, S. J. (2017). Varieties, production, composition and health benefits of vinegars: A review. *Food Chemistry*, *221*, 1621–1630. https://doi.org/10.1016/j.foodchem.2016.10.128
- Jana, P. K., Sarkar, S., & Chaudhuri, B. K. (2007). Maxwell–Wagner polarization mechanism in potassium and titanium doped nickel oxide showing giant dielectric permittivity. *Journal of Physics D: Applied Physics*, 40, 556–560. https://doi.org/10.1088/0022-3727/40/2/033
- Jeans, J. H. (1905). On the partition of energy between matter and Æther. *Philosophical Magazine, Series* 6, 6(10), 91-98. https://doi.org/10.1080/14786440509463348
- Kadiroğlu, P. (2018). FTIR spectroscopy for prediction of quality parameters and antimicrobial activity of commercial vinegars with chemometrics. *Journal of the Science of Food and Agriculture*, 98(11), 4121–4127. https://doi.org/10.1002/jsfa.8929
- Kassim, M. S., & Sarow, S. A. (2020). Flows of viscous fluids in food processing industries: A review. *Materials Science and Engineering*, *870*, Article 012032. https://doi.org/10.1088/1757-899X/870/1/012032
- Lambert, J. H. (1760). *Photometria, sive de mensura et gradibus luminis,* colorum et umbrae. Leipzig: Engelmann.
- Laun, M., Auhl, D., Brummer, R., Dijkstra, D. J., Gabriel, C., Mangnus, M. A., Rüllmann, M., Zoetelief, W., & Handge, U. A. (2014). Guidelines for checking performance and verifying accuracy of rotational rheometers: Viscosity measurements in steady and oscillatory shear. *Pure and Applied Chemistry*, 86(12), 1945–1968. https://doi.org/10.1515/pac-2013-0601
- Liu, Q., Tang, G. Y., Zhao, C. N., Gan, R. Y., & Li, H. B. (2019). Antioxidant activities, phenolic profiles, and organic acid contents of fruit vinegars. *Antioxidants*, 8, Article 78. https://doi.org/10.3390/antiox8040078
- Liu, Q., Zhong, Z., Wang, S., & Luo, Z. (2011). Interactions of biomass components during pyrolysis: A TG-FTIR study. *Journal of Analytical and Applied Pyrolysis*, 90, 213–218. https://doi.org/10.1016/j.jaap.2010.12.009

- Londonio, A., Morzán, E., & Smichowski, P. (2019). Determination of toxic and potentially toxic elements in rice and rice-based products by inductively coupled plasma-mass spectrometry. *Food Chemistry*, *284*, 149–154. https://doi.org/10.1016/j.foodchem.2019.01.104
- Lynch, K. M., Zannini, E., Wilkinson, S., Daenen, L., & Arendt, E. K. (2019). Physiology of acetic acid bacteria and their role in vinegar and fermented beverages. *Comprehensive Reviews in Food Science and Food Safety, 18*, 587–625. https://doi.org/10.1111/1541-4337.12440
- Macdonald, J. R. (1992). Impedance spectroscopy. *Annals of Biomedical Engineering*, *20*, 289–305. https://doi.org/10.1007/BF02368532
- Mach, E. (2003). *The principles of physical optics: An historical and philosophical treatment* (Original work published 1926). Dover Publications.
- Malisuwan, S., & Sivaraks, J. (2013). Frequency-dependent smith-chart model as applied to integrated circuit package antenna design. *International Journal of Computer and Communication Engineering*, *2*, Article 625. https://doi.org/10.7763/IJCCE.2013.V2.262
- Mazzer, H., Cardozo-Filho, L., & Fernandes, P. R. G. (2018). Broadband dielectric spectroscopy of protic ethylammonium-based ionic liquids synthetized with different anions. *Journal of Molecular Liquids*, 269, 556–563. https://doi.org/10.1016/j.molliq.2018.08.076
- Nguyen, Q. H., & Nguyen, N. D. (2012). Incompressible Non-Newtonian fluid flows. In Continuum mechanics –Progress in fundamentals and engineering applications (pp. 47–72). InTech. https://doi.org/10.5772/26091
- Okutan, M., Coşkun, R., Yalçın, O., Babuçoğlu, A. C., & Demir, A. (2023). Investigation of the dielectric and optic properties of rosehip seed extract loaded hydrogels. *Journal of Molecular Structure*, 1274(2), Article 134480. https://doi.org/10.1016/j.molstruc.2022.134480
- Okutan, M., Coşkun, R., Öztürk, M., Yalçın, O., & Toker, C. (2021). Equivalent circuit properties of organic food extracts doped hydrogels and their applications in bioelectronics. *Journal of Molecular Liquids*, *337*, Article 116401. https://doi.org/10.1016/j.molliq.2021.116401
- Okutan, M., Öztürk, M., Okutan, S., Yesilot, G., Yalçın, O., Bablich, A., & Bolívar, P. H. (2024). Impedance characterization of hydrothermally synthesized nickel zinc ferrite nanoparticles for electronic application. *Physica E: Low-dimensional Systems and Nanostructures*, *158*, Article 15900. https://doi.org/10.1016/j.physe.2024.115900
- Owen, T. (1996). *Fundamentals of UV-visible spectroscopy: A primer* (Technical Publication No. 12:5965-5123E, pp. 14–25). Hewlett-Packard Company.
- Öztürk, M. (2021a). Evaluation of quality the pumpkin, wild plum, pear, cabbage traditional homemade vinegars using the spectroscopy and rheology methods. *Spectrochimica Acta Part A: Molecular and Biomolecular Spectroscopy*, 259, Article 119896. https://doi.org/10.1016/j.saa.2021.119896
- Öztürk, M. (2021b). Determination of quality in homemade vinegars by spectroscopy and rheology methods. *Düzce University Journal of Science & Technology*, 9, 1493–1506. https://doi.org/10.29130/dubited.882634
- Öztürk, M., Yalçın, O., Tekgündüz, C., & Tekgündüz, E. (2022). Origin of the effects of optical spectrum and flow behaviour in determining the quality of dry fig, jujube, pomegranate, date palm and concentrated grape vinegars. *Spectrochimica Acta Part A: Molecular and Biomolecular Spectroscopy*, 270, Article 120792. https://doi.org/10.1016/j.saa.2021.120792
- Padmamalini, N., & Ambujam, K. (2016). Impedance and modulus spectroscopy of ZrO₂– TiO₂–V₂O₅ nanocomposite. *Karbala International Journal of Modern Science*, *2*, 271–275. https://doi.org/10.1016/j.kijoms.2016.10.001
- Rayleigh, L. (1900). LIII. Remarks upon the law of complete radiation. *Philosophical Magazine*, *49*(301), 539–540. https://doi.org/10.1080/14786440009463878
- Ríos-Reina, R., Callejón, R. M., Oliver-Pozo, C., Amigo, J. M., & García-González, D. L. (2017). ATR-FTIR as a potential tool for controlling high quality vinegar categories. *Food Control*, *78*, 230–237. https://doi.org/10.1016/j.foodcont.2017.02.065
- Routray, W., & Orsat, V. (2014). Variation of dielectric properties of aqueous solutions of ethanol and acids at various temperatures with low acid concentration levels. *Physics and Chemistry of Liquids*, *52*, 209–232. https://doi.org/10.1080/00319104.2013.812022
- Singh, A., Singh, A., Singh, S., Tandon, P., Yadav, B. C., & Yadav, R. R. (2015). Synthesis, characterization and performance of zinc ferrite nanorods for room temperature sensing applications. *Journal of Alloys and Compounds*, 618, 475–483. https://doi.org/10.1016/j.jallcom.2014.08.190
- Smith, P. H. (1939). Transmission line calculator. *Electronics*, 12, 29-41.
- Tauc, J. (1968). Optical properties and electronic structure of amorphous Ge and Si. *Materials Research Bulletin*, *3*, 37–46. https://doi.org/10.1016/0025-5408(68)90023-8

- Ubeda, C., Callejón, R. M., Hidalgo, C., Torija, M. J., Mas, A., Troncoso, A. M., & Morales, M. L. (2011). Determination of major volatile compounds during the production of fruit vinegars by static headspace gas chromatography–mass spectrometry method. *Food Research International*, *44*, 259–268. https://doi.org/10.1016/j.foodres.2010.10.025
- Vu, T. T. N., Teyssedre, G., Roy, S. L., & Laurent, C. (2017). Maxwell-wagner effect in multi-layered dielectrics: Interfacial charge measurement and modelling. *Technologies*, *5*, 1–15. https://doi.org/10.3390/technologies5020027
- Wagner, K. W. (1914). Erklarung der dielektrischen nachwirkungsvorgange auf grund maxwellscher vorstellungen. *Archiv für Elektrotechnik*, *2*, 371–387. https://doi.org/10.1007/BF01657322
- Wang, L., Yang, J., Lin, Q., Xiang, L., Song, Z., Zhang, Y., & Chen, L. (2019). Determination of 10 organic acid contents in tea using high performance liquid chromatography-diode array detector. *Journal of Zhejiang University: Agriculture and Life Sciences*, 45, 47–53. https://doi.org/10.3785/j.issn.1008-9209.2017.12.192
- Williams, D. H., & Fleming, I. (1989). Spectroscopic methods in organic chemistry (pp. 12–85). McGraw Hill Inc.
- Yalçın, O., Öztürk, M., & Görgülüer, Ö. (2022). Investigation of optical and flow properties of avocados by spectroscopy and rheology methods. *Acta Physica Polonica A*, 141, 481–486. https://doi.org/10.12693/aphyspola.141.481
- Yalçın, O., Tekgündüz, C., Öztürk, M., & Tekgündüz, E. (2021). Investigation of the traditional organic vinegars by UV–VIS spectroscopy and rheology techniques. *Spectrochimica Acta Part A: Molecular and Biomolecular Spectroscopy, 246*, Article 118987. https://doi.org/10.1016/j.saa.2020.118987